Engineering and Technology Journal
Journal homepage: https://etj.uotechnology.edu.iq

Numerical Investigation of a Window Solar Air Collector with Moveable Absorber Plates

Norhan I. Dawood *, Jalal M. Jalil, Majida K. Ahmed

Electromechanical Engineering Dept, University of Technology-Iraq, Alsina'a Street, 10066 Baghdad, Iraq.
*Corresponding author Email: eme.19.37@grad.uotechnology.edu.iq

HIGHLIGHTS

- A new novel window with 7 movable absorber plates with different opening angles.
- Best thermal performance and minimum of sunlight were obtained at angle 0°.
- Lower thermal performance and maximum of sunlight were obtained at angle 90°.
- A flexibility between hot air and sunlight requirements for angles between 0 and 90°.

ARTICLE INFO

Handling editor: Muhsin J. Jweeg

Keywords:
Circular perforated plate
moveable absorber plate
solar simulator
window solar air collector

ABSTRACT

Window solar air collector is an imperative instrument for heating residential buildings in cold regions. This paper presents a numerical investigation of the thermal performance of a window solar air collector with seven moveable absorber plates. With glass on the front and back sides of the collector. By the use of FORTRAN 90; The three-dimensional steady-state turbulent forced convection method was used to solve the Navier-Stokes equations. The seven plates opened and closed at different angles in unison manually by a specific mechanical mechanism. The effect of changing the plate angles has been tested, alongside the effect of airflow rates and the intensity of solar radiation. Numerical results illustrate that air temperature difference is higher at vertical plates position (angle 0°) compared to that at angle 90. In contrast, flexibility between sunlight penetrating the room and hot air from the collector will be gained when the plates are set on angle 90. Results indicate that the thermal performance was improved by 67% when the plates were set at angle 0. Maximum thermal efficiency for angle 0 was 72% at a mass flow rate of 0.0298 kg/s. However, maximum thermal efficiency was 51% at mass flow rate 0.0298 for angle 90°.

1. Introduction

Thermal solar collectors are an advantageous approach of utilizing the solar energy as a renewable energy source. As the solutions being employed and elaborated for the last decades and can be divided into solar collectors that use water as well as solar collectors that use air. Solar water collectors have a more regularly a preference for preparing hot water or preheating the thermal agent needed for heating. On the contrary, thermal solar air collectors are employed to reheat air which is in request for heating, drying, etc. Contrasted to the water collectors, air collectors have the prevalence of preventing any risk of freezing besides, these systems have lesser impact on the environment [1].

Moshfegh and Sandberg [2] analyzed numerically the fluid flow and heat transfer characteristics of buoyancy-driven convection between two vertical parallel walls, heated from one side. A steady-state two-dimensional model is used for the analysis. The numerical investigation led to two conclusions. First of all, it improved understanding of the heat transfer mechanism in a vertical channel that is heated from one side. As the investigation revealed the significance of radiation heat exchanges in the mechanisms of heat transfer between the channel walls. Furthermore, it covered the computational tool, and it was successful in obtaining numerical results for natural convection in a vertical channel heated from one side. Philips et al. [3] obtained a numerical resolution of the integrate free radiative and convective heat transfer from an isothermal window conjoins to a venetian blind made of aluminum. The results indicate that a venetian blind possesses a significant impact on the rate of heat transfer from indoor glazing surface. The mentioned blind was detected to significantly reduce the rate of radiative heat transfer from the window. There were two competing impacts observed for convection. When fixing an aluminum blind near a window, the slats with a high conductivity will act as an extended surface, enhancing convection. The blind, on the other hand, inhibits

http://doi.org/10.30684/etj.v40i7.2270
Received 1 July 2021; Accepted 28 August 2021; Available online 20 May 2022
2412-0758/University of Technology-Iraq, Baghdad, Iraq

free convective flow close to the window surface, that reduces the rate of heat transfer. Liao et al. [4] offered a CFD study of fluid flow and heat transfer in a photovoltaic thermal system integrated into a building designed for single-story applications. The coefficients of heat transfer for the two cavity surfaces were predicted, and the convective coefficient was specified using a combination of CFD simulations and experimental measurements with boundary conditions. Velocity profiles experimental measurements in the BIPV system cavity employing a particle image velocimetry system were in good agreement with CFD model predictions. Han et al. [5] provided numerical solving and explanations for the energy and Navier–Stokes equations for natural convection laminar flow in the air duct cavity of a window system with double pane and an inserted visional PV glass. As it was detected that convective flow increases as well as heat transfer being enhanced with the increment in Rayleigh number. This research affords precise heat transfer variables that are required for concluding the conversion efficiency of the PV taking into consideration the temperature of the solar cell and inspecting the thermal performance of building elements integrated with PV, like a transparent PV double-pane window. The results indicate that employing a PV double pane window with a low-e coating minimize a significant amount of heat transfer by radiation within the air cavity. Li et al. [6] investigated numerically and experimentally the air flow and heat transfer characteristics of a solar air collector with glazed, transpired, and slit like perforations. At constant plate porosity and through the slit like perforated plate, local resistance loss is less than that through circular holes. They discovered that for limited heat capacities, as air volume rate exceeds 160 m^3/h, the increment in fan power surpasses the increase in heat collected, along with a declination in the effective efficiency. The effective efficiency enhances with the increase in the diameter of perforations and ambient temperature. Besides, it decreases in the plenum thickness, pitch and inlet air temperature. Jalil et al. [7] analyzed numerically micro pin fins impact on the performance of heat transfer. As the equations of Navier-Stokes were solved by 3-D turbulent forced convection and steady-state. Numerous numbers of micro pin fins accompanied by in line configuration as well as multi micro pin fins configurations like staggered configuration supplementary to the in-line configuration were discussed. Michaux et al. [8] investigated numerically the thermal performance of a window with a triple glazed airflow. As numerical and experimental conclusions present that the air supply being preheated via the airflow window is remarkable, with temperatures ranging between 10–20 °C with no solar irradiance and within sunny times. Numerical results indicate that, because of the fresh outdoor air being entered, therefore, the present window induce a heavy cold wall effect. Simultaneously, it minimizes cold draught risks (approximately 10 °C air supply preheating) as well as heat losses. In fact, due to same reasonings, the airflow through the window glazing has a low outer face temperature and consequently external heat transfers occurs through convection and radiation declined. Hu et al. [9] examined experimentally and numerically the system's thermodynamic behavior. The system is designed to enhance indoor air quality and thermal comfort by supplying continuous pre-heated air at a low energy cost by capturing and storing solar energy. They demonstrated a PCM solar air heat exchanger integrated into a ventilated window, which was designed to make the most efficient use of solar energy to pre-heat the ventilated air. When there is enough solar energy, it charges the PCM solar air collector. The ventilated window receives ventilation air, which is pre-heated by solar radiation.

The majority of the researchers concentrated on the improvement of the thermal efficiency of the solar air collectors. Thus, a numerical investigation of compromising between the hot air gain and sunlight penetration to the desired room is needed. Therefore, a window solar air collector with glass on the front and back sides is presented as it could be used in residential buildings and homes to provide part of the heating load during cold weather. Generally, it will reduce the use of traditional heaters as well. For these reasons, it is essential to design a new SAC that would fully fulfil the space heating requirement. This paper aims to interrogate the numerical performance of window solar air collector with circular perforated absorber plates as the present collector will supply both hot air and sunlight to the desired place. The mechanism of combining circular perforations and the flat plate is put forward alongside moveable absorber plates.

2. CFD modeling and Numerical analysis

2.1 Assumptions

For the purpose of analyzing and construct the mathematical model of the governing equations of the window solar air collector, it can be clarified under the following assumptions:

1) The flow in the present study is considered 3-D, incompressible, and at a steady state.
2) Turbulent flow is considered through the collector.
3) At average temperature, all properties are evaluated.
4) Heat transfer by forced convection.
5) Uniform distribution of irradiance on the glass cover.
6) Body forces are negligible.
7) Inlet air temperature is equal to the ambient temperature.
8) All properties are taken at room temperature.

2.2 Governing equations and applied boundary conditions

The airflow inside the window solar air collector is turbulent, 3-D, continuous, and incompressible. Navier Stokes equations (NSEs) (continuity, momentum, and energy) were solved by the use of control volume (SIMPLE algorithm) in order to be built in the program by FORTRAN90. The SIMPLE algorithm is an iterative procedure for the calculation of pressure and velocity fields **[10]**. The 3-D turbulent NSEs write the eq name with forced convection in Cartesian coordinates; after simplification the equations will be:

2.2.1 Momentum Equations

X-direction

$$\frac{\partial U^2}{\partial x}+\frac{\partial UV}{\partial y}+\frac{\partial UW}{\partial z}=-\frac{1}{\rho}\frac{\partial P}{\partial x}+\frac{\partial}{\partial x}\left(\nu e\frac{\partial U}{\partial x}\right)+\frac{\partial}{\partial y}\left(\nu e\frac{\partial U}{\partial y}\right)+\frac{\partial}{\partial z}\left(\nu e\frac{\partial U}{\partial z}\right)+\frac{\partial}{\partial x}\left(\nu e\frac{\partial U}{\partial x}\right)+\frac{\partial}{\partial y}\left(\nu e\frac{\partial V}{\partial x}\right)+\frac{\partial}{\partial z}\left(\nu e\frac{\partial W}{\partial x}\right) \quad (1)$$

Y-direction

$$\frac{\partial UV}{\partial x}+\frac{\partial V^2}{\partial y}+\frac{\partial VW}{\partial z}=-\frac{1}{\rho}\frac{\partial P}{\partial y}+\frac{\partial}{\partial x}\left(\nu e\frac{\partial V}{\partial x}\right)+\frac{\partial}{\partial y}\left(\nu e\frac{\partial V}{\partial y}\right)+\frac{\partial}{\partial z}\left(\nu e\frac{\partial V}{\partial z}\right)+\frac{\partial}{\partial x}\left(\nu e\frac{\partial U}{\partial y}\right)+\frac{\partial}{\partial y}\left(\nu e\frac{\partial V}{\partial y}\right)+\frac{\partial}{\partial z}\left(\nu e\frac{\partial W}{\partial y}\right) \quad (2)$$

Z-direction

$$\frac{\partial UW}{\partial x}+\frac{\partial VW}{\partial y}+\frac{\partial W^2}{\partial z}=-\frac{1}{\rho}\frac{\partial P}{\partial z}+\frac{\partial}{\partial x}\left(\nu_e\frac{\partial W}{\partial x}\right)+\frac{\partial}{\partial y}\left(\nu_e\frac{\partial W}{\partial y}\right)+\frac{\partial}{\partial z}\left(\nu_e\frac{\partial W}{\partial z}\right)+\frac{\partial}{\partial x}\left(\nu_e\frac{\partial U}{\partial z}\right)+\frac{\partial}{\partial y}\left(\nu_e\frac{\partial V}{\partial z}\right)+\frac{\partial}{\partial z}\left(\nu_e\frac{\partial W}{\partial z}\right) \quad (3)$$

2.2.2 Energy Equation

$$\frac{\partial UT}{\partial x}+\frac{\partial VT}{\partial y}+\frac{\partial WT}{\partial z}=\frac{\partial}{\partial x}\left(\Gamma_e\frac{\partial T}{\partial x}\right)+\frac{\partial}{\partial y}\left(\Gamma_e\frac{\partial T}{\partial y}\right)+\frac{\partial}{\partial z}\left(\Gamma_e\frac{\partial T}{\partial z}\right) \quad (4)$$

The general form of the Navier Stokes equations after simplification the equations will be:

$$\frac{\partial}{\partial x}(\rho U\phi)+\frac{\partial}{\partial y}(\rho V\phi)+\frac{\partial}{\partial z}(\rho W\phi)=\frac{\partial}{\partial x}\left(\Gamma_\phi\frac{\partial\phi}{\partial x}\right)+\frac{\partial}{\partial y}\left(\Gamma_\phi\frac{\partial\phi}{\partial y}\right)+\frac{\partial}{\partial z}\left(\Gamma_\phi\frac{\partial\phi}{\partial z}\right)+S_\phi \quad (5)$$

As the first term on the left represent convection term whereas the one on the right represents both diffusion and source terms, respectively. As Φ is the dependent variable, and S_Φ is the source term for various governing equations.

Where:

$$\Gamma_k=\nu_t/\sigma_k \quad (6)$$

$$\Gamma_\epsilon=\nu_t/\sigma_\epsilon \quad (7)$$

And

$$\Gamma_u=\Gamma_v=\Gamma_w=\mu_{eff} \quad (8)$$

$$\mu_{eff}=\mu+\mu_t \quad (9)$$

$$\mu_t=c_\mu\rho\frac{k^2}{\epsilon} \quad (10)$$

Table 1: Source terms in the governing (PDEs)

Equation	**Φ**	Γ_Φ	S_Φ
Continuity	1	0	0
U-momentum	U	Γ_u	$-\frac{\partial P}{\partial x}+\frac{\partial}{\partial x}\left(v_e\frac{\partial U}{\partial x}\right)+\frac{\partial}{\partial y}\left(v_e\frac{\partial V}{\partial x}\right)+\frac{\partial}{\partial z}\left(v_e\frac{\partial W}{\partial x}\right)$
V-momentum	V	Γ_v	$-\frac{\partial P}{\partial y}+\frac{\partial}{\partial x}\left(v_e\frac{\partial U}{\partial y}\right)+\frac{\partial}{\partial y}\left(v_e\frac{\partial V}{\partial y}\right)+\frac{\partial}{\partial z}\left(v_e\frac{\partial W}{\partial y}\right)$
W-momentum	W	Γ_w	$-\frac{\partial P}{\partial z}+\frac{\partial}{\partial x}\left(v_e\frac{\partial U}{\partial z}\right)+\frac{\partial}{\partial y}\left(v_e\frac{\partial V}{\partial z}\right)+\frac{\partial}{\partial z}\left(v_e\frac{\partial W}{\partial z}\right)$
Temperature	T	Γ_e	0
Kinetic Energy	K	Γ_k	G-ε
Dissipation Rate	ε	Γ_ε	$C_{1\varepsilon}\frac{\varepsilon}{k}G-C_{2\varepsilon}\frac{\varepsilon^2}{k}$

Table 2: The empirical constants for (k- $\boldsymbol{\varepsilon}$)

C_μ	$C_{1\varepsilon}$	$C_{2\varepsilon}$	σ_k	σ_ε
0.09	1.44	1.92	1.00	1.30

2.2.3 Initial conditions

The WSAC integrated with 7 moveable absorber plates as the system is initially believed to be at ambient temperature of $T_{am} = 25\ °C$:

Both front and back glass covers, lower and upper absorber surfaces:

$T = T_{amb}$

2.2.4 Boundary conditions

The boundary conditions for the entire system composed of:

a) At the collector cover, glass on the front and back sides and lower and upper absorbing surfaces, and the side edge walls; (U=V=W=0), no slip condition.

b) Inlet boundary conditions For inlet temperature:

$At\ x = 0 \quad , \ T = T_{in} \ , \ U = U_{in}$

For turbulence parameters:

$$k_{in} = C_k u_{in}^2 \tag{11}$$

$$\varepsilon_{in} = C_\mu k_{in}^{3/2} / (0.5 D_h C_\varepsilon) \tag{12}$$

Where C_k and C_ε are the constants of ($C_k = 0.003$, $C_\varepsilon = 0.03$).

c) Outlet boundary conditions

In the outlet section, a fully developed flow included the set normal gradients to be zero, which can be written as:

$At\ x = 0, \quad \frac{\partial \Phi}{\partial x} = 0$

Where;

Φ….. referred to independent variables of: $U,\ W,\ V, T, k\ and\ \varepsilon$.

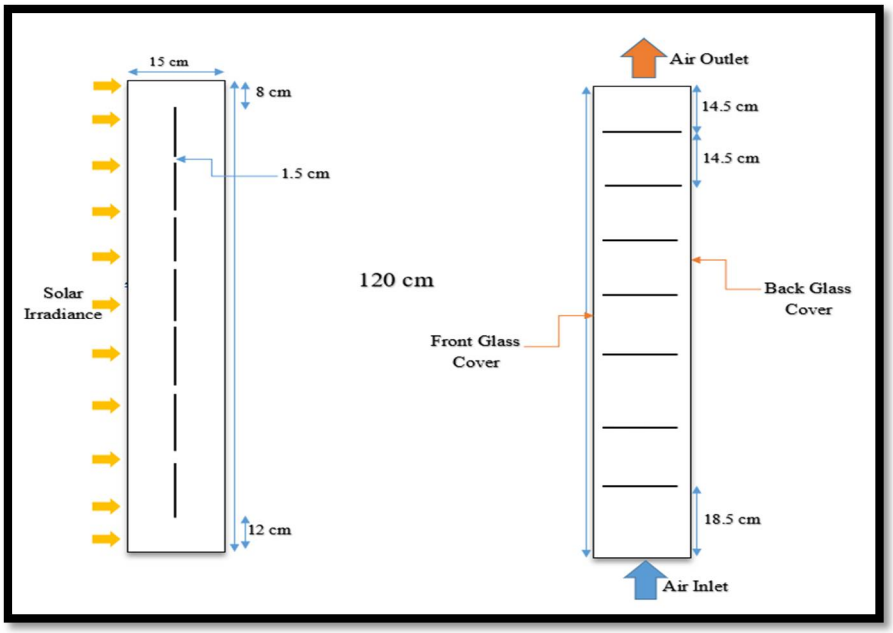

Figure 1: Side view of WSAC when the plates set at angle 0° and at angle 90°

3. Results and Discussion

The performance of the suggested window solar air collector with seven moveable absorber plates was studied numerically for angles 0 and 90, employing a modified FORTRAN 90 program. The effect of varying the intensity of solar radiation and airflow rate was considered as the results of the numerical analysis were discussed with several parameters. The same statuses of the experimental device of window solar air collector Dawood et al. 2021 [11] were applied in this numerical works. A total of 24 cases with different airflow and irradiance were studied. To calculate the velocity vectors, the Navier Stoke Equations were solved.

Figures 2 and 3 illustrate the effect of air flow rate on the temperature difference between inlet and outlet air when the plates are in a full close position (angle 0) and a fully open position (angle 90). Increasing solar radiation intensity will lead to an increase in the temperature difference of air. However, increasing the mass flow rate will decline the temperature difference due to reducing the contact time between the plates and the flowing air inside the collector. Moreover, the solar radiation falling on a particular area when the plates opened at angle 90; on the contrary, when the plates closed at angle 0, the solar radiation is fully absorbed by the plates. As the area of the incident solar flux at angle 0 is much greater than at angle 90.

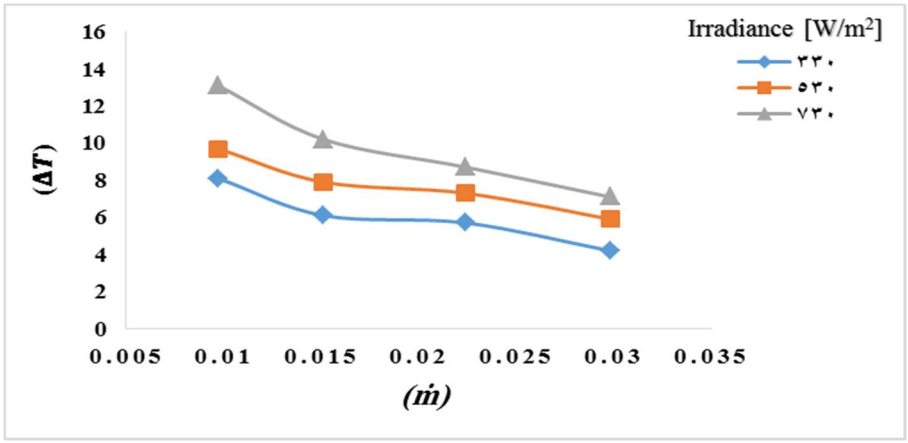

Figure 2: Variation of temperature difference of air flow with mass flow rate at various irradiance at angle 0°

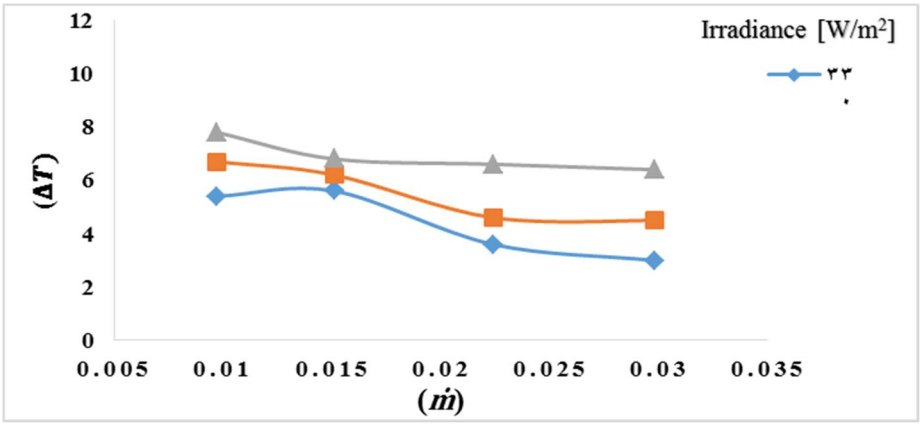

Figure 3: Variation of temperature difference of air flow with mass flow rate at various irradiance at angle 90°

Figure 4 and Figure 5 demonstrate the difference between numerical and experimental results Dawood et al. [11], for the temperature difference between the air inlet and outlet for angles 0° and 90°, respectively. These figures show a reasonable agreement between the numerical and experimental results. By contrasting the numerical and experimental details, it is evident that the results of the numerical study are higher than the experimental results by a small margin due to the neglect of the losses.

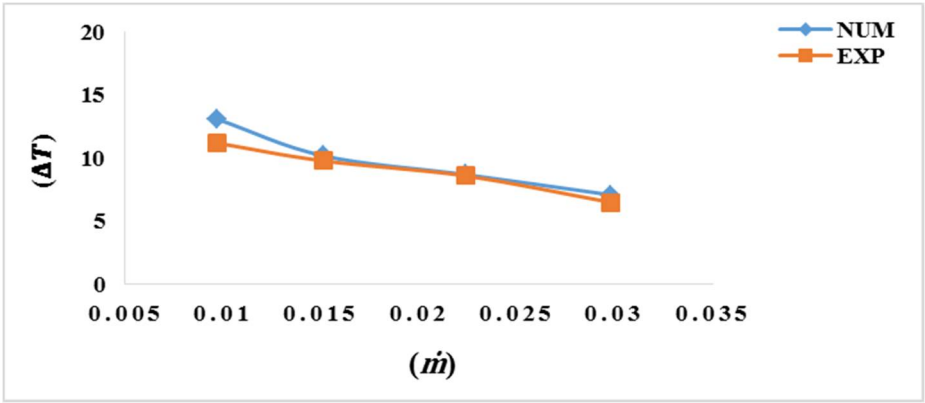

Figure 4: Experimental and Numerical variations of outlet air temperature of WSAC at irradiance =730 W/m^2 for angle 0°

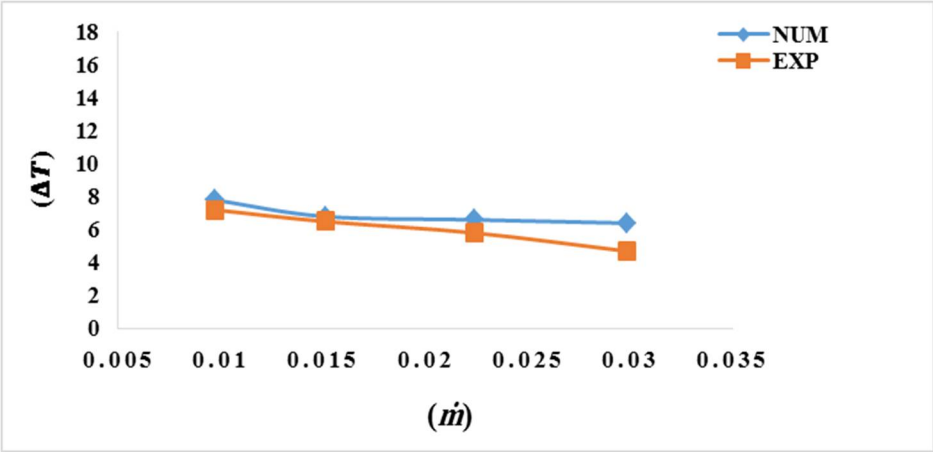

Figure 5: Experimental and numerical variations of outlet air temperature of WSAC at irradiance =730 W/m^2 for angle 90°

Figure (6) demonstrates the numerical variation of the thermal efficiency that had been tested of window solar air collector as a function of air flow rate and a specific solar intensity for both angles 0° and 90°. As it can be seen, the thermal efficiency of the collector enhanced by increasing inlet mass flow rate. The highest thermal efficiency was calculated as 62% in mass flow rate 0.0298 kg/s and at plates set vertically at angle 0°. While the maximum thermal efficiency gained for angle 90° was 47% for the same mass flow rate and solar intensity.

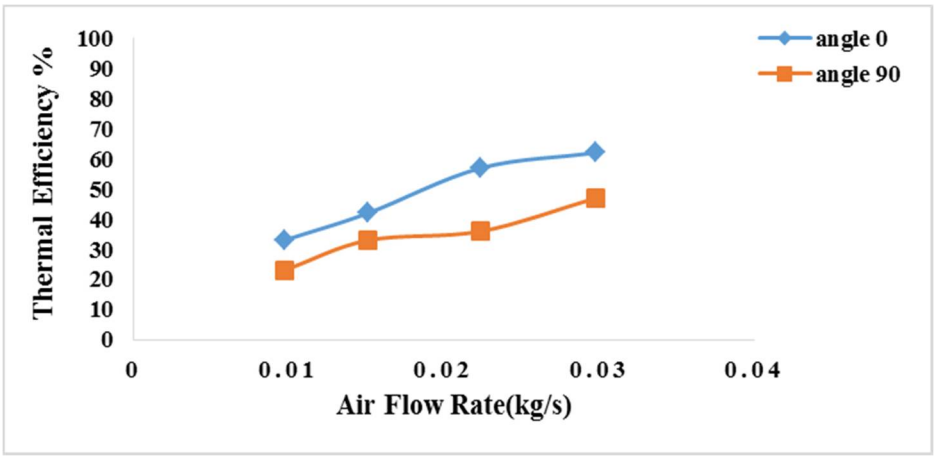

Figure 6: Thermal efficiency of angle 0° and angle 90° with mass flow rate of WSAC at irradiance =530 W/m^2

Figure 7 (a, b) and Figure 8 (a, b) display the contours of temperature were plotted in three- dimensional form, demonstrating temperature gradient along the collector duct at a mass flow rate of 0.0097 kg/s and irradiance 730 W/m^2. Air passes through the absorber plates and gains a portion of thermal energy. It is noticeable that the direction of temperature increases towards the flow along the channel. Figure 7 (a), and Figure 8 (a) related to angle 0°, which show the increase of temperature across the collector channel due to the hot elements which are the plates and the hot glass body surrounding the air flow. However, in angle 90° case, Figure 7 (b), and Figure 8 (b) illustrate that the temperature growth is less than that in angle 0°,due to the solar radiation distribution on the plates. Moreover, that the air flow temperature in the collector channel decrease near the back glass especially in angle 0° case, that would be due to the position of the absorber plates that allow the solar radiation to penetrate to the back glass only through the circular perforations on the plates body. Figure 9 (a, b) shows the flow field in the window solar air collector at angles 0° and 90° as 3D at a mass flow rate of 0.0224 kg/s and irradiance 730 W/m^2. The velocity decreased as pointing towards the collector duct walls till becoming zero at the walls for both angles. From Figure (9, b**),** it was notable that the air velocity is almost zero when it hits the solid plate in the case of angle 90°, while the airspeed through only the circular perforations on the plate. On the other hand, in the case of angle 0° as shown in Figure (9, a), air flows smoothly over the absorber plates. That led to a higher air velocity in the case of angle 0° comparing to angle 90°. while Figure (10, c), and (10, d) show the side view of the flow field for the collector for the same mentioned angles at a mass flow rate of 0.0224 kg/s and irradiance 730 W/m^2, it had been illustrated that the flow is smoothly flowing near the front and back glass cover walls, and the velocity decrease through the circular perforations.

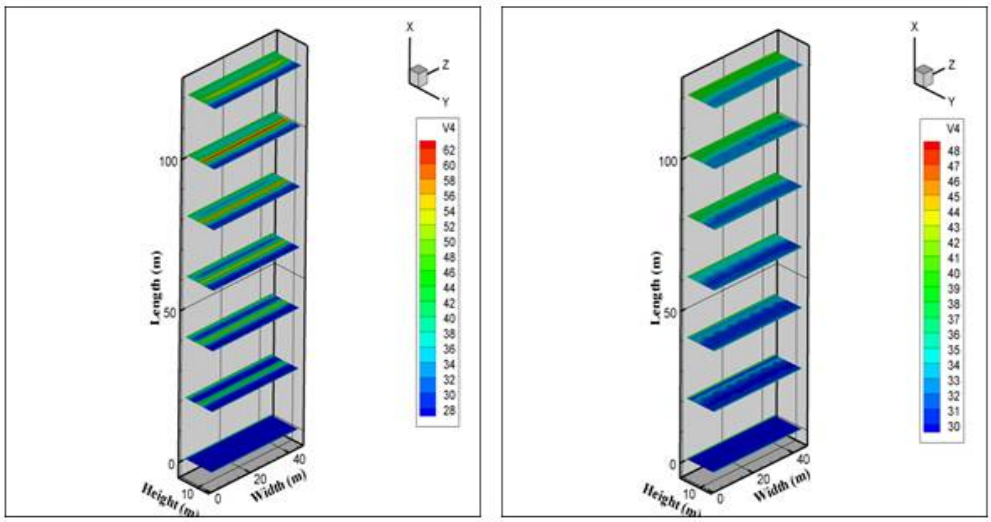

(a) Angle 0° **(b) Angle 90°**

Figure 7: Isotherm contours of WSAC, 3-D

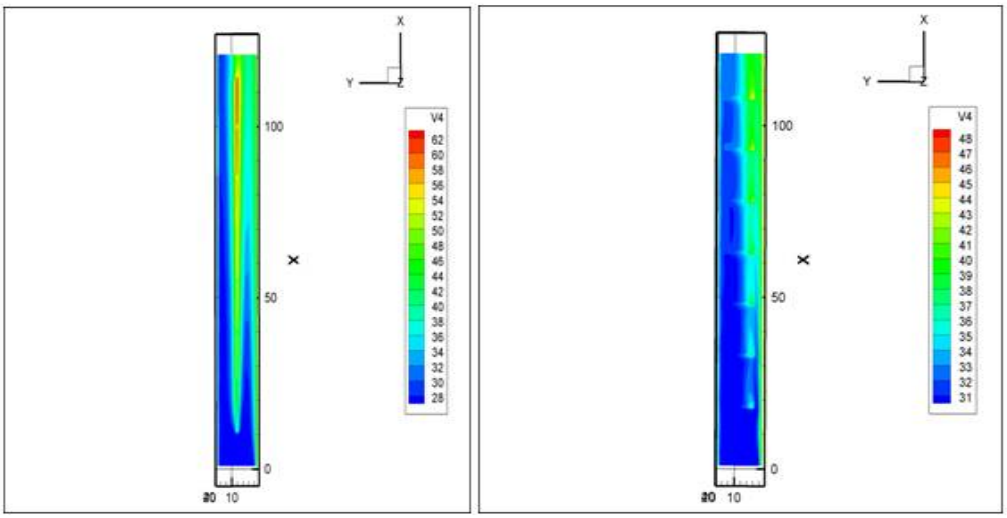

(a) Angle 0° **(b) Angle 90°**

Figure 8: Isotherm contours of WSAC, Side view

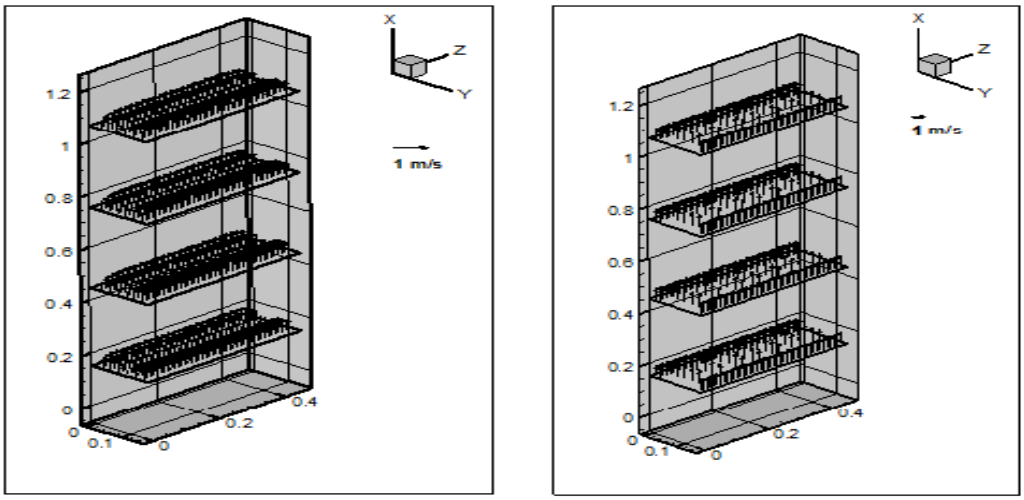

(a): Angle 0° **(b): Angle 90°**

Figure 9: Flow field in window solar air collector, 3-D

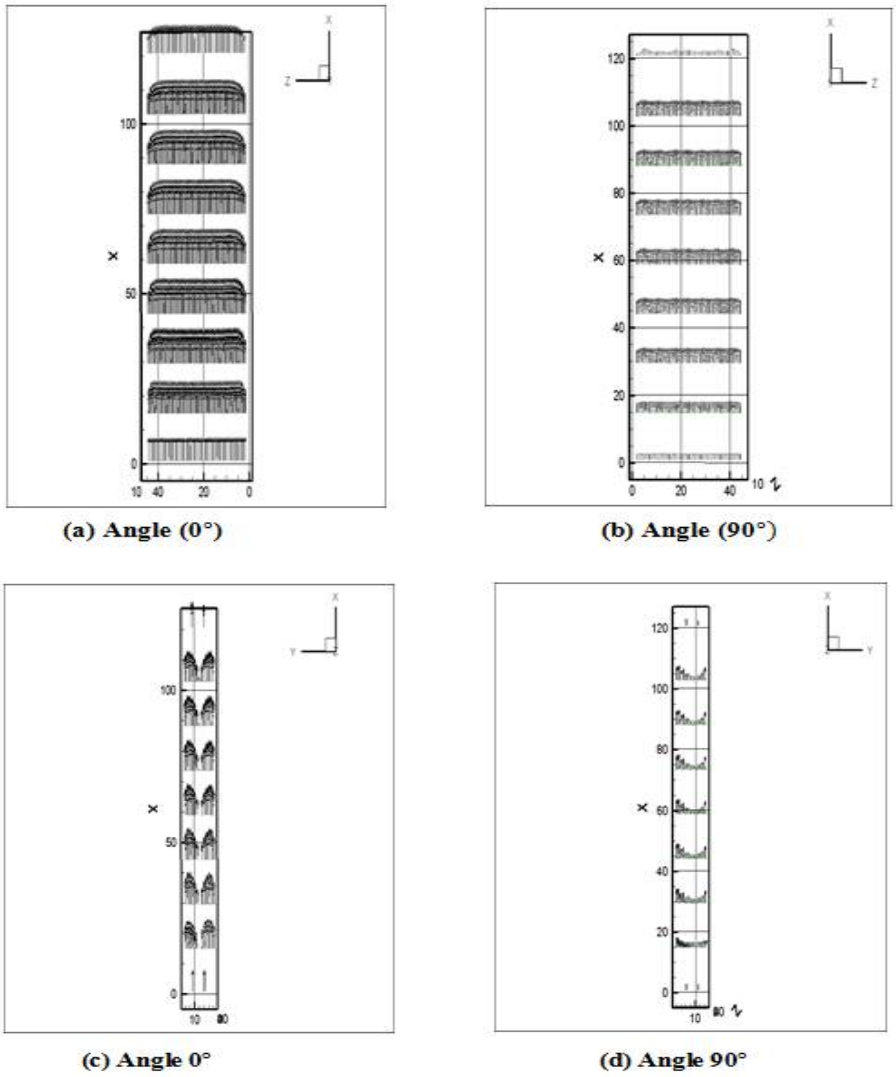

Figure 10: Flow field in window solar air collector, front and side view

4. Conclusions

In this study, the effect of air mass flow rate and solar intensity on the thermal performance of the window solar air collector with seven moveable absorber plates was investigated numerically. The study is beneficial for popularizing and applying solar air collectors in cold regions and during cold weather. The main conclusions of the present study can be summarized as:

1) The present window solar air collector is a new type of solar collectors that provide both hot air and sunlight to the residential building, by controlling the movement of the absorber plates manually to be opened in different angles, two angles were taken into consideration, which is 0° and 90°.
2) The thermal performance is enhanced when the plates are positioned vertically at angle 0°; it will represent the usual shape of a solar collector and provide hot air only with sunlight penetration through the circular perforations on the plate surface to the room.
3) As the plates are set at angle 90°, the sunlight will be fully penetrated through the glass cover to the desired place with less heating than angle 0°. As the thermal performance was enhanced by 67% when the plates were set at angle 0°.
4) Maximum thermal efficiency was gained at angle 0° which is equal 71%, on the other hand maximum thermal efficiency for angle 90° were 56%.
5) Comparing the numerical and experimental results showed a good agreement. The average difference between the numerical and experimental data is 8 %, which indicates that the thermal model is correct and reliable.

Nomenclature

T_{out} , T_{in}	Outlet and inlet air temperature (℃)
U, V, W	Velocity in (x, y, and z) directions (m/s)
Γ	Diffusion coefficients (kg/m sec)
S_Φ	Source term
Φ	Any of the variables needed to be solved
K	Thermal conductivity (W/m.K)
ε	Dissipation rate of turbulent kinetic energy
$C_{1\varepsilon}, C_{2\varepsilon}, C_k$	Constants in turbulence model
$\sigma_k, \sigma_\varepsilon$	Turbulent Prandtl numbers for K, ε
$a_n, a_s, a_e, a_w, a_t, a_b$	Coefficients in general Finite- Volume equations
i, j, k	Indices that express positions in the (x,y,z) directions
k	Kinetic Energy

Author contribution

All authors contributed equally to this work.

Funding

This research received no specific grant from any funding agency in the public, commercial, or not-for-profit sectors.

Data availability statement

The data that support the findings of this study are available on request from the corresponding author.

Conflicts of interest

The authors declare that there is no conflict of interest.

References

[1] A. S. Bejan, A. L., C. Croitoru1* and T. Catalina, Air solar collectors in building use - A review , E3S Web of Conf., 01003, 32 , 2018. https://doi.org/10.1051/e3sconf/20183201003

[2] M. Sandberg, and B. Moshfegh, Investigation of fluid flow and heat transfer in a vertical channel heated from one side by PV elements, part I-Numerical study, J. Renew. Energy, 8 (1996) 248-253. https://doi.org/10.1016/0960-1481(96)88857-4

[3] J. Phillips, D. Naylor, P. H. Oosthuizen, and S. J. Harrison, Numerical study of convective and radiative heat transfer from a window glazing with a venetian blind, HVAC&R Res., 7 (2001).

[4] L. Liao, A. K. Athienitis, L. Candanedo, K. W. Park, Y. Poissant, and M. Collins, Numerical and experimental study of heat transfer in a BIPV-thermal system, Sol. Energy Eng., 129 (2007) 423-430. https://doi.org/10.1115/1.2770750

[5] J. Han, L. Lu, and H. Yang, Numerical evaluation of the mixed convective heat transfer in a double-pane window integrated with see-through a-Si PV cells with low-e coatings, ACS Appl. Energy Mater., 87 (2010) 3431-3437. https://doi.org/10.1016/j.apenergy.2010.05.025

[6] X. Li, C. Li, and B. Li, Net heat gain assessment on a glazed transpired solar air collector with slit-like perforations, Appl. Therm. Eng., 99 (2016) 1-10. https://doi.org/10.1016/j.applthermaleng.2015.12.069

[7] J. M. Jalil, A. H. Reja, and A. M. Hadi, Numerical Investigation of Thermal Performance of Micro-Pin Fin with Different Arrangements, IOP Conf. Series: Mater. Sci. Eng., 765 (2020) 012037, IOP Publishing.

[8] G. Michaux, R. Greffet, P. Salagnac, and J. B. Ridoret, Modelling of an airflow window and numerical investigation of its thermal performances by comparison to conventional double and triple-glazed windows, ACS Appl. Energy Mater., 242 (2019) 27-45. https://doi.org/10.1016/j.apenergy.2019.03.029

[9] Y. Hu, P. K. Heiselberg, H. Johra, & R. Guo, Experimental and numerical study of a PCM solar air heat exchanger and its ventilation preheating effectiveness, J. Renew. Energy, 145 (2020) 106-115. https://doi.org/10.1016/j.renene.2019.05.115

[10] H. K. Versteeg and W. Malalasekera, An introduction to computational fluid dynamics: the finite volume method, Pearson education, second ed, uk, (2007).

[11] N. I. Dawood, J. M. Jalil, and M. K. Ahmed, Experimental Investigation of a Window Solar Air Collector with Circular-Perforated Moveable Absorber Plates, the 3rd int. Sci. conf. Eng. Sci. adv. Technol., (IICESAT), Iraq, (2021), Paper 83, Unpublished.